**High degree of optical tunability of self-assembled photonic-plasmonic crystals by filling fraction modification**

By *Martín. López-García*[1], *Juan Francisco. Galisteo-López*[1],*Álvaro. Blanco*[1], *Cefe López*[1*] and *Antonio García-Martín*[2]

[1] M. López-García, J.F. Galisteo-López, A. Blanco, J. Sánchez-Marcos, C. López are with Instituto de Ciencia de Materiales de Madrid (CSIC) and Unidad Asociada CSIC-U. Vigo C/ Sor Juana Inés de la Cruz 3, 28049 Madrid (Spain). E-mail: cefe@icmm.csic.es

[2] A. García Martín, Instituto de Microelectrónica de Madrid (IMM-CSIC), C/ Isaac Newton 8, 28760 Tres Cantos, Madrid (Spain)

Keywords: Plasmonics, photonics, emission, tunability.

## Abstract

The optical properties of two-dimensional hybrid photonic-plasmonic crystals are fine-tuned by modifying the dielectric component of the system. The filling fraction of the dielectric component in monolayers of spheres deposited on gold substrates is controlled by means of oxygen plasma etching. In doing so we are able to spectrally tune the optical modes of the system. Experiments are performed on both, optically passive and active samples showing the possibility to strongly modify the emission properties of samples containing an emitter distributed within the spheres. The change in sphere diameter needed to substantially modify the sample's optical response points to a potential use of these samples as sensors or tunable emitting devices if appropriate polymeric components are employed.

## 1. Introduction

Among the possible approaches to attain a control over light propagation at the nano/microscale, plasmonic and photonic crystals have become two of the most powerful techniques. Surface plasmon resonances (SPR) provide very large and localized field enhancement, integrability with microelectronics or supertransmisison phenomena.[1] On the other hand photonic crystals (PCs) have demonstrated novel routes for light control by means of density of states (DOS) engineering including full photonic bandgaps [2] or strong modification of spontaneous emission in two-dimensional (2D) and 3D systems.[3,4] However, some intrinsic problems related with these new structures have not yet been solved. On the one hand SPRs present very short propagation lengths hampering their use in large area devices. On the other hand organic PCs, attractive from the point of view of applications as well as for the ease and low cost of fabrication, lack the large refractive index contrast needed for experimentally realizing strong DOS modifications. A possible avenue to circumvent such limitations and obtain the best out of the above two systems would be their combined use in hybrid structures. Recent results have shown that coupling between waveguided modes associated with dielectric structures and plasmonic resonances may lead to laser devices in the nanoscale.[5] Also exploiting hybrid plasmonic-photonic systems, SPR supporting metallic structures can be loaded with structured organic materials. In this way, hybrid plasmonic-waveguided modes can be tailored to obtain large propagating lengths along with field enhancements larger than those in their dielectric counterparts.[6,7] A step further can be taken if the dielectric-metallic interface is modulated achieving a PC structure. The latter system sustains modes propagating in the dielectric part that could be used, for instance, to obtain enhanced emission of internal sources.[8,9] Among all the available techniques to obtain such a modulation in/over the metallic structure, monolayers of self-assembled colloidal nano-spheres is one of the most useful ones thanks to the large area,[10] good crystalline quality and straightforward fabrication.[11] Typically used as templates for more complex structures in plasmonics[12] the possibility of using these structures as PCs

has also been demonstrated.[13] Recently it has also been shown[7,9,14,15,16,17] that when such PCs are grown over a metallic film supporting SPR hybrid photonic-plasmonic modes can be found with strong field enhancement at different spatial positions in the sample.

The functionality of the above described plasmonic-photonic systems could be certainly enhanced by changing its optical response under an external stimulus, turning them into tunable devices. Among the several strategies to do this, modifying the plasmonic modes optically,[18] electrically,[19] magnetically[20][21] or acoustically[22] can be counted. Alternatively one can modify the refractive index or lattice constant of the organic lattice to tailor the photonic dispersion and hence the optical response of the system.[23] Certain stimuli could even be employed to simultaneously tune both types of modes and the hybrid ones arising from them.

In this work we present an easy to implement processing method to tune the optical response of the hybrid modes of self-assembled monolayers of polymeric spheres deposited on metallic films. For these systems, we have recently shown how we can exploit the redistribution of the total field intensity to strongly modify the spontaneous emission of internal sources.[9] The tuning of their optical response is obtained by homogeneously reducing each sphere while keeping the lattice parameter constant, i.e. by changing the filling fraction of the hexagonal lattice as studied before for PCs on dielectric substrates.[24]. In the present work we have used polystyrene (PS) spheres. Two diameters (0.52 and 1 μm) were tested for which the three kind of modes, namely, waveguided-like (WG) plasmon-like (SPP) and hybrid ones, fall in the visible-NIR range.[9] By means of oxygen plasma etching each sphere of the monolayer is reduced in its entire volume in a controlled way while maintaining its lattice position. It is well known that isotropic oxygen plasma etching constitutes an ideal method to reduce polymeric colloidal particles. This method has been used to modify the diameter of spheres forming monolayers on dielectric substrates [25] as well as to locally change the filling fraction of 3D opal based PhC to improve coupling to slow modes[26] and to introduce planar defects.[27] This fine tuning was applied to close-packed monolayers deposited on thin gold films (60 nm). In this way the system

modes can be modified in a controlled manner and experimentally monitored by means of VIS-NIR reflectance measurements. Experimentally observed blueshifts of the modes were measured and accounted for with numerical simulations. At the same time, the modification of the modal spatial profile was numerically studied in order to evaluate changes on field confinement within the structure. As a step further, the same process was applied to samples grown from dye doped spheres for which enhanced emission at those frequencies matching the modes of the system has been previously reported.[9] Emission spectra were collected after each etching step and it was found that changing the sample geometry upon etching strongly modifies the spontaneous emission of internal sources. The tuning process presented in this work is a non reversible one and, therefore, suited for fine-tuning the optical response of the system during the fabrication process. However active devices based on the same principle could be obtained. Typical changes in diameter obtained (*ca.* 100 nm, i.e. 10% of sphere diameter) could be achieved with certain hydrogels as has been already demonstrated for 3D self-assembled structures. Hence, we believe the present method could be implemented in the future with similar materials, in order to develop a fully tunable emitting device in which changes over directionality or polarization can be attained.

## 2. Results and discussion

Characterization prior to the etching process is required in order to estimate the filling fraction (*ff*) reduction of the lattice attained as a function of plasma time. Filling fraction is defined here as the ratio between the volume occupied by polystyrene divided by the volume of the unit cell of the lattice. Etching was performed on monolayers (sphere diameter $\phi$ = 1 μm) for increasing plasma times. Scanning electron microscopy (SEM) at each etching step allowed to obtain the sphere diameter. Two examples can be found in the insets of **Fig. 1**, corresponding to different points in the calibration graph. From the images it can be observed that, after each treatment, the sample retains a good crystalline quality and that the lattice parameter is larger than the

diameter of the spheres. We can define a shrinkage parameter $\gamma = \phi/\phi_0$ to describe the etching. Thus we can express the filling fraction as $ff = \gamma^3\pi/3\sqrt{3}$.

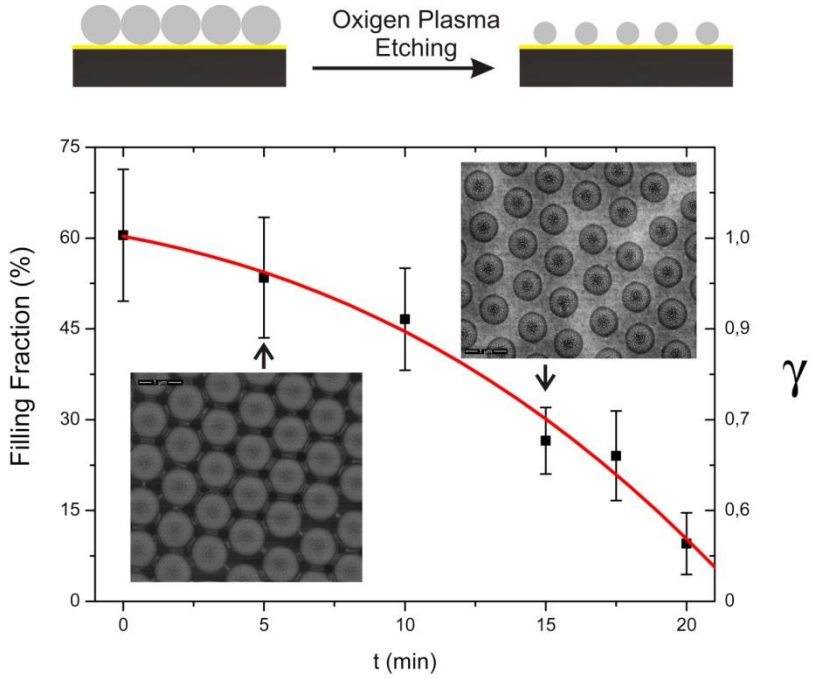


**Figure 1.** Plasma-etching reduction of $\Phi_0$ = 1 µm PS spheres over a 20 minute period. Insets show SEM images for the same sample at two different etching times: 5 (bottom) and 15 (top) minutes. γ stands for the ratio between the final diameter ($\Phi_f$) and the original $\Phi_0$ one. The red line fits to thirth degree polynomial.

From the calibration plot of Fig. 1 we can obtain the etching rate in this case for 1 µm diameter spheres. The reduction process is not a linear one, as would be expected from previous studies[28] and if we take into account the fact that spheres in a close-packed configuration should be less affected by the plasma. That is, the etching ratio in the initial stages should be smaller than when the spheres have been appreciably shrunk. During the initial 10 minutes of etching in which we go from the close packed lattice (*ff* = 0.60 for the monolayer case) to a *ff* ~ 0.44, the reduction rate can be considered almost linear with a slow PS removing rate (~ $\Delta\gamma$ = 0.01 per minute) for 1µm spheres. For longer treatments, PS etching is much faster. SEM images show that the crystalline quality of the lattice remains good during the first 15 minutes of etching time. For longer reduction times, spheres may lose its sphericity making a more complex anisotropic etching technique necessary.[25] Given that large diameter reductions are not the aim of this work (since optical quality can be severely damaged) we will concentrate in the initial

slow linear reduction range. Though the amount of PS removed should be the same independently of sphere size, it is advisable that an etching calibration to obtain the *ff* reduction be performed for each sphere size under study. In our case a study was also carried out for the $\phi$ = 520 nm spheres in the initial linear-like region.

In order to track the evolution of the optical response as homogenous sphere reduction takes place, normal reflection spectra where collected for a monolayer of $\phi$ = 1μm spheres from the close packed lattice until a 100 nm diameter reduction (γ= 0.9 ).

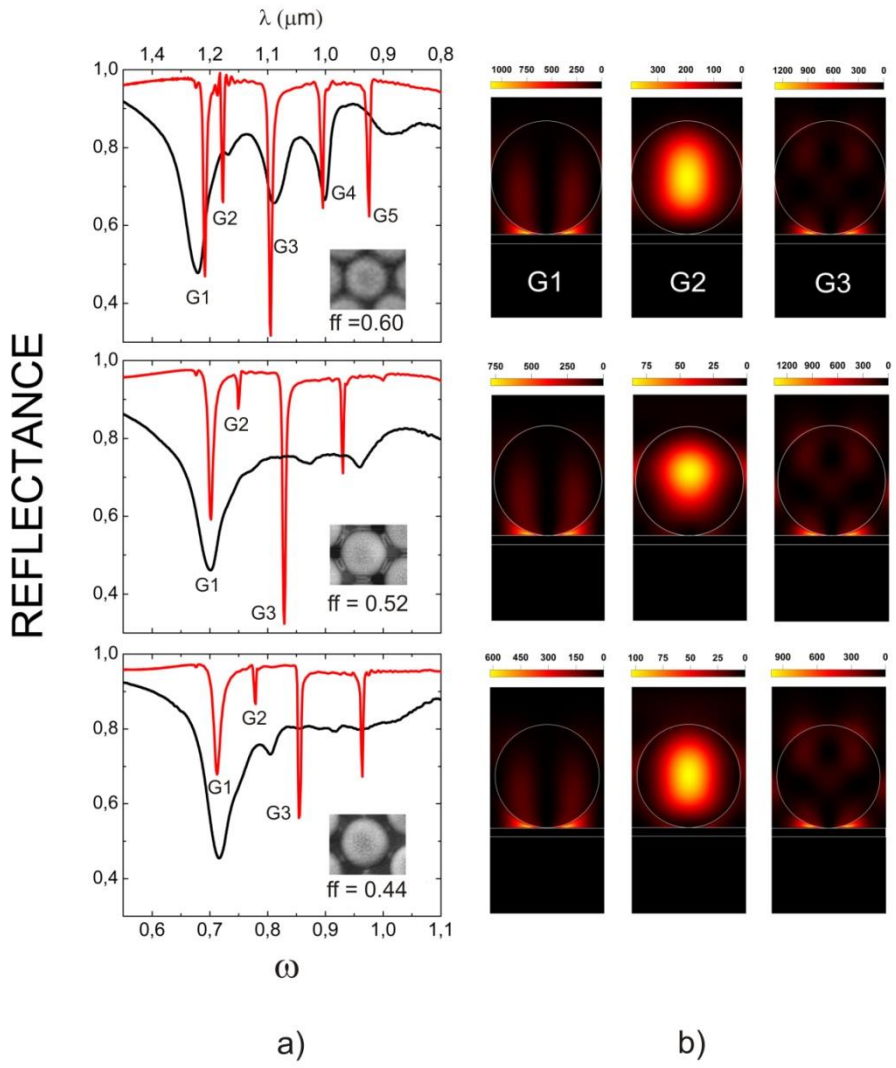


**Figure 2.** a) Normal incidence reflectance for three different filling fractions. Top to bottom: ff = 0.6, ff = 0.52 and ff = 0.44 corresponding to γ = 1.00.52, γ = 0.95 and $\gamma$ = 0.90, 50 and 100 nm respectively. Experimental (black) and theoretical spectra (red) are presented. b) Total field intensity distribution and its evolution with sphere resizing for the first three modes in the left panel.

**Fig. 2** shows both experiment and simulated far field reflectance for three different sphere diameter. As explained before,[9,12,15] this kind of systems support hybrid modes along with the

plasmonic resonances (SP modes) provided by the metallic film and the photonic modes (WG modes) provided by the periodic structure of the monolayer of dielectric spheres. The five large dips shown in the reflectance spectra correspond to modes of the sample. Coupling efficiency as well as field enhancement will be dependent on the nature of each mode. For this study we will consider the first three modes (G1 to G3), representative of the three types of modes sustained by these systems, although the same behavior is obtained for the other two modes available (G4 and G5).

A good overall agreement between simulations and experimental data can be found. However, some differences for spectral width and position of the peaks can be observed, most likely, due to residual disorder introduced during the growing process. Polydispersity of the spheres can be a source for defects too though, in our case, its effect should not be very important due to the small values for the present spheres (less than 3% according to the manufacturer).

In order to characterize the modal distribution of the system, the total field intensity spatial distribution in the sample was numerically obtained. Fig. 2b shows simulations when the structure is illuminated at normal incidence at those frequencies matching the G1, G2 and G3 modes. For the maximum filling fraction ($\gamma = 1$ or ff = 0.6), G1 and G3 show a large SP-like character with a large field enhancement at the gold film surface, the main difference between the two modes being the field pattern within the sphere. For the G2 mode the field intensity remains mainly concentrated inside the spheres, indicating a WG-like nature. When $\gamma = 0.95$ ($ff = 0.52$) is achieved, all modes are blue shifted. This is a consequence of the reduction in the effective refractive index of the dielectric region over the gold film as the sphere volume fraction is reduced. On the one hand, SPR propagation is strongly dependent on the dielectric constant of the surrounding medium[1] and a reduction of the effective index of the metallic film loading material will spectrally shift SPRs to higher energies. On the other hand, WG-like mode profile is determined by the size and shape of the spheres which dramatically change when the filling fraction of the total lattice is reduced [13,24] If we examine the total field distribution of the

different modes as the filling fraction is reduced we can see that the WG or SP character of the modes remains unchanged and only a slight decrease of the field is observed.

While results for only three etching steps have been shown above, the procedure can be carried out in a continuous manner allowing a fine degree of control of the sample topology and hence its optical response. To show this, reflectance spectra where recorded over a 12.5 minute period in 30 seconds etching steps, which corresponds to the first linear reduction region shown in Figure 1. As a result, $\phi$= 1μm spheres where reduced as much as 100 nm in diameter (0.46 < *ff* < 0.60). Theoretical spectra calculated like those in Fig 2 were obtained for the same diameters. For the experimental case, an initial diameter of $\phi$ = 1020 nm was considered in order to match the theoretical spectra, probably a consequence of the 3% polydispersity of the spheres. Nevertheless, the filling fraction reduction was comparable in both cases. The two reflection maps obtained for simulations and experiments are plotted in **Fig. 3**.

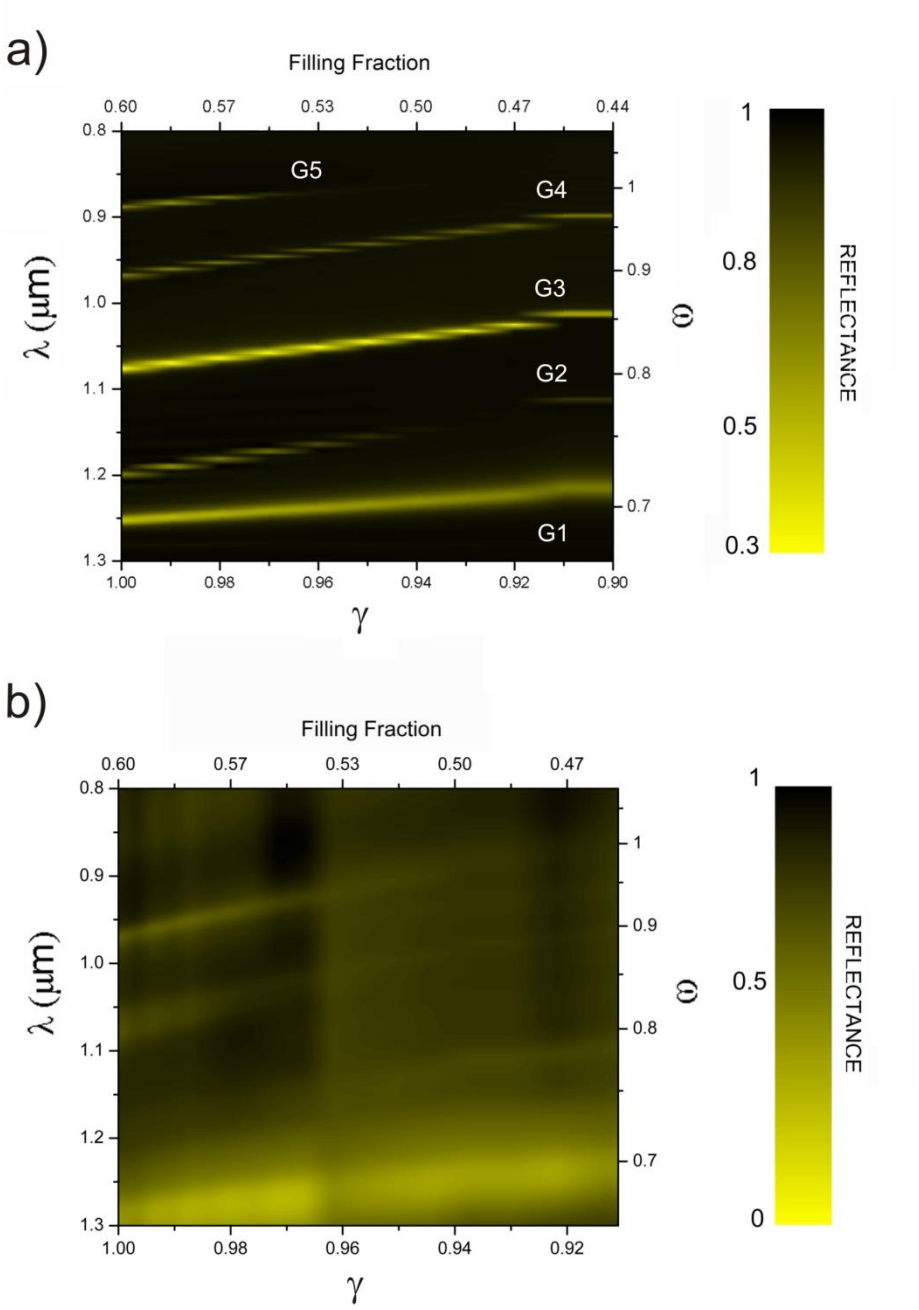


**Figure 3.** Calculated (a) and experimental (b) reflectance spectra represented as a contour plot for a monolayer of $\phi$= 1μm spheres as the filling fraction is varied from the close-packed lattice (*f f*= 0.6) to one with a 100 nm reduction in diameter (*ff* = 0.44).

Fig. 3a shows that as the filling fraction of the sample is reduced, the optical response undergoes two major changes. On the one hand there is an overall blue shift of the modes attributed, as already discussed, to a decrease in the effective index of the dielectric part of the system. On the other hand there is a change in the intensity of the dips in the reflectance spectra. While those modes having a marked SP character (G1, G3) hardly change, those with a WG or hybrid

character (G2, G4 and G5) present strong variations in intensity. This fact indicates that for the latter modes, when we reduce the sphere diameter, the spatial distribution of the field undergoes strong changes as already seen in the mode profiles of figure 2. A clear example is seen for the case of G2, where for a sphere reduction $\gamma = 0.94$ the associated dip all but vanishes and then recovers upon further reduction. Accompanying this result is the increase of ca. an order of magnitude in the field intensity inside the spheres (see Fig.2).

When measurements are compared with calculations a good agreement is found. Modes G1, G3 and G4 present an identical linear blue shift with *ff* reduction in both cases. Some differences are appreciated for experimental mode position at *ff* below 0.5. This is due to the fact that plasma reduction rate becomes slightly higher as the spheres are reduced, reaching a rate larger than the initial one. For the close-packed structure, G2 can be hardly appreciated due to the proximity of G1 which presents a very broad and intense dip, hiding the real value for reflectance at $\omega$=0.71. However, it is possible to see that for *ff* = 0.47 ($\gamma = 0.92$) its coupling efficiency rises as was expected from theoretical results.

As a last analysis of modes evolution, it is observed in Fig 3a that spectral shift of the resonances is linear with sphere diameter reduction. This fact is useful from the point of view of tuning several systems fabricated from the same initial spheres. Once the ratio has been estimated for one sample we can use optical characterization as a means to control the tuning of the optical response of the rest without recourse to SEM inspection[25] which would slow down the process of tuning the optical features to given requirements Furthermore, the rates obtained (0.04 in average for the different modes) could be slowed down or speeded up depending on the conditions of the plasma process.

So far we have considered the tunability of the optical response of optically passive samples with the diameter of the spheres. As an application, the same tuning strategy has been adopted to modify the emission properties of a similar sample with luminescent properties. In this case we have used dye (Rodamine 6G) doped $\phi$ = 520 nm spheres. The diameter was chosen in

order to overlap the dye's broad band emission spectrum with the G2, G3 modes of the pristine spheres structure. Close-packed samples were subject to an etching process for up to 7.5 min (corresponding to $\gamma = 0.88$ nm or a final $ff = 0.41$). Etching times were chosen in order to restrict ourselves to the linear reduction rate region, as in $\phi = 1\mu m$ case. **Figure 4** shows normal incidence reflectance and emission spectra for three different steps of the etching process. The close packed structure shows the same modes as the $\phi = 1\mu m$ sample only not so well defined. This is due to the proximity of the optical features to the absorbance region of the gold film. Indeed, some difference in spectral mode position may happen due to the strong dispersion of gold in the new spectral range under study. Despite that, numerical simulations (not shown) demonstrate that the conclusions about modal evolution observed for the larger sphere samples are still valid in this case.

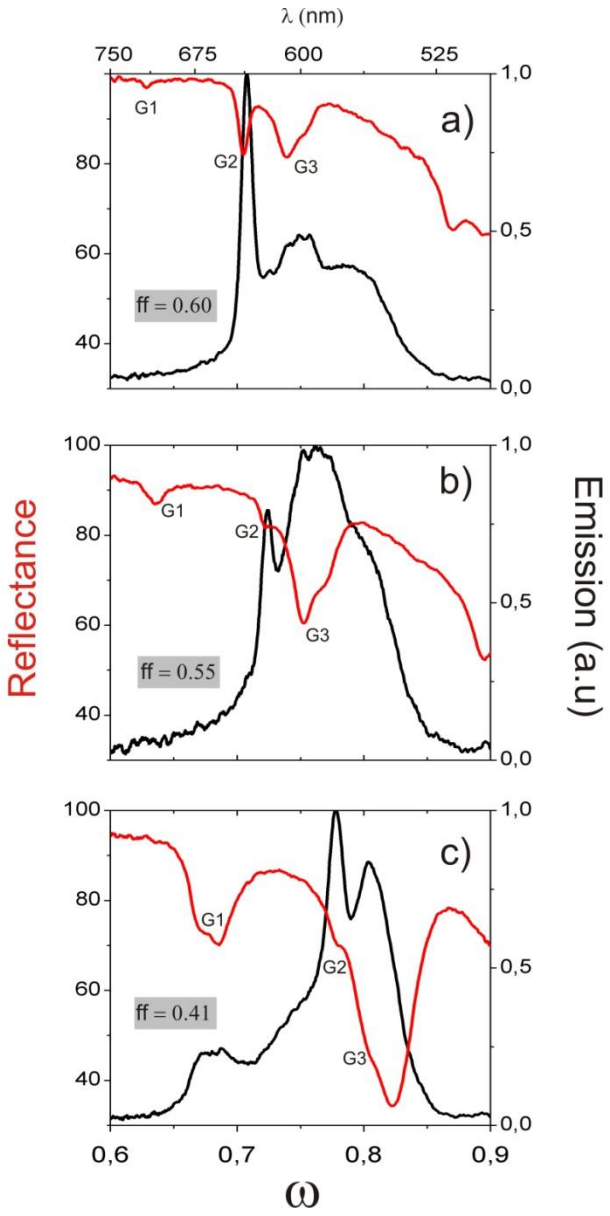


**Figure 4**. Normal incidence reflectance (red) and emission (black) spectra for $\phi$= 520 nm dye doped spheres at three different filling fractions corresponding to: γ = 1 (a), γ = 0.97 (b) and $\gamma = 0.88$ $(c)$.

Emission for disordered dye doped spheres (no photonic-plasmonic effect) presents its maximum at 610 nm with 70 nm spectral width. When the spheres are structured into a close-packed lattice, emission can be strongly enhanced for those frequencies spectrally matching a mode of the structure.[9] In particular the WG-like mode (G2) is the most suitable to enhance the dye's emission given that its field profile matches the geometrical position of the dye molecules in the structure (inside the sphere). **Figure 4a** (close packed sample, *ff* = 0.6) shows how a strong emission enhancement takes place for ω = 0.71, corresponding to the G2 mode. Emission

enhancement for *ff*=0.6 also takes place at $0.73 < \omega < 0.78$, associated with mode G3. For G1 no enhancement is present due to the fact that it is spectrally far from the emission of the dye.

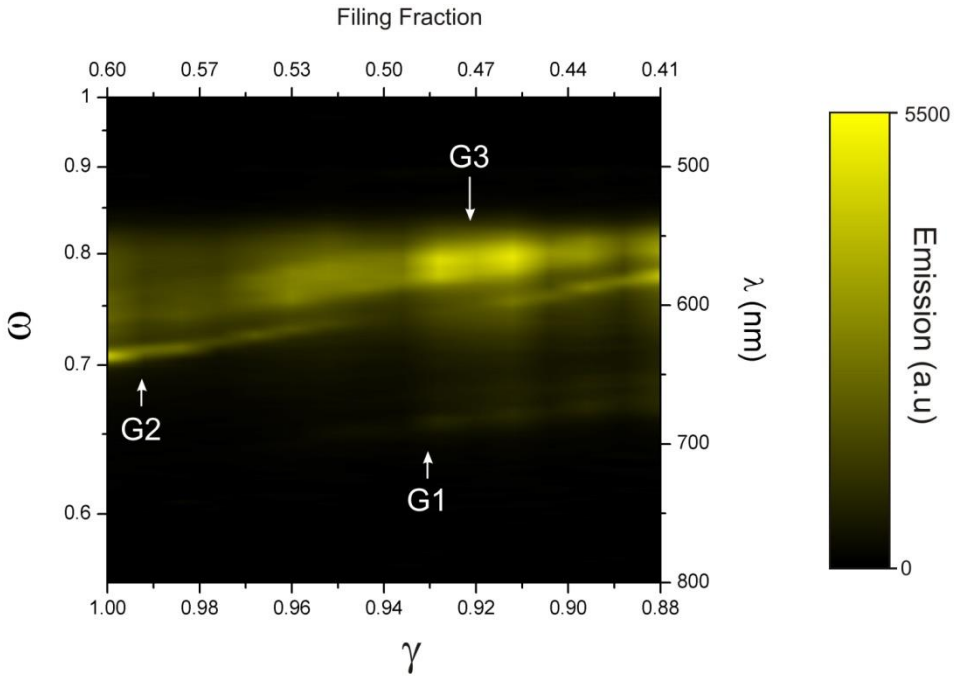


**Figure 5.** Emission (in arbitrary units) as a contour plot for a monolayer of $\phi$= 520 nm dye doped PS spheres in a continuous filling fraction reduction process. Oxygen plasma etching was carried out from the close packed scenario (ff = 0.60) to a final filling fraction of ff = 0.41.

When diameter of the spheres is reduced under plasma etching the blue shift of the modes in reflectance, already studied for the $\phi$ = 1 μm case, is also observed only in the visible spectral range now. Upon comparison of reflection and emission spectra (Fig. 4) it is evident that the peaks of enhanced emission follow the trend of dips in reflection, corresponding to the modes of the structure. In this way one can effectively tune the sample's emission by controlling the plasma process. Beside the spectral shift, changes in the magnitude of emission enhancement taking place as the etching process advances are a combination of two factors. The first one can be associated to the variations in the field confinement taking place as we reduce the sphere diameter (see discussion above and Fig. 2) and the second to the fact that, as the reduction process takes place, the modes of the system are swiped across the dye's broad emission so that

enhanced emission should be more probable the closer a mode is to the dye's emission maximum.

A clear example of the above is that of mode G1, of SPP-like character. While for *ff* = 0.6 (Fig. 4a) no enhanced emission takes place at the spectral position of this mode (ω=0.62) owing to the fact that it is far from the dye's emission, as we decrease the sphere diameter we shift its spectral position until for γ = 0.95 it eventually overlaps the dye's emission (*ff* ≈ 0.51 ). At that point emission enhancement is already visible; moreover it is clear that as γ reduces and the mode blue shifts, the emission increases as can be seen for *ff*= 0.41 and ω=0.68 in Fig. 4c. The fact that such enhancement is not as large as for the other modes is now due to the small spatial overlap between the dye and the field (mainly concentrated near the gold surface). Finally it must be noted that as the etching process takes place the effects of disorder, broadening the peaks in reflection, becomes more evident. This fact is likely responsible for the discrepancy between reflection and emission of the G3 peak in the case of the smallest filling fraction (Fig. 4c). Here the peak in reflectance broadens considerably and causes a part of the peak to fall in the high energy tail of the emission (where it is less efficient) and hence causing an asymmetry of the emission peak.

As was done for the $\phi$ = 1μm spheres with reflectance measurements, a map of the emission of the $\phi$ = 520 nm spheres has been collected as the sphere size is reduced in small steps (see Fig. 5). Here several facts are worth mentioning. Firstly, we can trace the evolution of mode G2 and see that as we reduce the sphere diameter we can continuously shift its spectral position but also modulate its intensity taking it to a minimum for γ ≈ 0.94 (*ff* = 0.49). For even larger diameter reductions we see how it recovers its intensity. For the case of the SPP-like G1 mode it is now clearly seen how it appears as an enhancement in emission for γ ~ 0.95 nm, as we shift it towards the dye's emission. Finally mode G3 is also seen to blue shift and reach a maximum as it overlaps the highest value of the dye's emission for a *ff* = 0.47. Nevertheless, the behavior observed in emission for the $\phi$ = 520 nm qualitatively matches that observed in reflection for

the $\phi$ = 1μm ones indicating that although we are considering different spectral regions, where the dielectric constant of gold changes, the system still presents acceptable scalability.

## 3. Conclusion

In conclusion, we have shown a straightforward method to fine tune the plasmonic/photonic hybrid modes of one monolayer of PS spheres deposited on a gold substrate. It has been demonstrated that a small reduction of filling fraction of the lattice produces large spectral blueshifts as well as variations on the spatial distribution of the total field intensity depending on the character (SPP-like or WG-like) of the mode studied. These changes are accompanied by a strong modification of the sample's optical response both in reflectance and emission when optically active spheres are used. Experimental results have been numerically modeled and a good agreement was found, which is remarkable since modal distribution has been found to be very sensitive to small changes in the structure's morphology. The easy and inexpensive method to finely tune the optical properties of the samples could find application in some active research fields such as organic emitting devices. Further, since the magnitude of the structural changes we have imprinted on our samples are similar to those achievable with tunable polymeric spheres made from hydrogels, these results could be applied as a proof of principle for future sensing devices where tunability is achieved by means of external stimuli.

## 4. Experimental

*Sample Fabrication*. Close-packed monolayers were fabricated by the vertical deposition method. [29] A rigid substrate was introduced vertically in a colloidal suspension with a controlled concentration (0.08 % wt.) low enough to produce just one sphere thick layer. The growth was performed in an oven under stabilized temperature (50ºC) and humidity (20%). We used commercial PS spheres (Duke Scientific) with two different diameters: 0.52 and 1 μm. The former ones had an organic dye (Rhodamine 6G) homogeneously distributed throughout

their volume. Their diameter was chosen to tune optical features to the appropriate spectral range in each case. The $\phi$ = 1μm spheres were chosen to tune the lowest energy mode (G1) to the NIR range and allow us to place as many higher energy modes as possible in the NIR-VIS range which is where the optical detectors we used (Si/InSb) performed best. One should take into account that when working at those wavelengths large negative real values of the dielectric constant of gold provide the best performance when SPP modes are considered. On the other hand, for $\phi$ = 520 nm, the condition was to overlap the four (G1 to G4) first modes with the dye's emission spectrum. As a substrate, we used 450 μm thick silicon wafers (ACM) on which a thin (60 nm) gold film was sputtered.

For spheres reduction a commercial oxygen plasma etching stripper (Tetra Pico from Diener Electronics) was used. The exposure time was controllable with a minimum etching step of 10 seconds.

*Optical measurements*. To optically characterize the sample two different set-ups were used. For normal incidence reflectance measurements in the NIR spectral range we used a Fourier Transform Infrared (FTIR) spectrometer coupled to a 4× microscope objective with a low Numerical Aperture (NA=0.1). For reflectance/emission spectra at visible wavelengths we used a large numerical aperture (NA=0.75) 40× microscope objective coupled to a microscope. Its output was collected by a 100 μm core optical fiber coupled to a portable spectrometer (Ocean Optics 2000+ USB).

*Simulations.* Numerical simulations were performed with commercial software (Lumerical FDTD Solutions) from which normal incidence reflectance spectra were calculated along with the spatial distribution of the total field intensity at those wavelengths where mode excitation takes place. The presence of the gold layer, together with the possible coupling to localized excitations makes it necessary to employ a fine grid (40 points per wavelength in each direction) as well as long enough simulation time.

Acknowledgements

The authors would like to acknowledge Jorge Sánchez-Marcos for providing high quality gold coated substrates. J.F. G-L was supported by the JAE Postdoctoral Program from the CSIC. M. L-G was supported by the FPI PhD program from the MICINN. This work was partially supported by EU FP7 NoE Nanophotonics4Energy grant No. 248855; the Spanish MICINN CSD2007-0046 (Nanolight.es), MAT2009-07841 (GLUSFA), CSIC PIF08-016 (Intramural Frontera) and Comunidad de Madrid S2009/MAT-1756 (PHAMA) projects. A. García-Martín also acknowledges financial support from the Spanish MICINN ("MAGPLAS" MAT2008-06765-C02-01/NAN, Funcoat Consolider Ingenio 2010 CSD2008-00023) and European Comission (NMP3-SL-2008-214107-Nanomagma).

**References:**

[1] W.L. Barnes, A. Dereux, T.W. Ebbesen, *Nature* **2003**, *424*, 824.

[2] A. Blanco, E. Chomski, S. Grabtchak, M. Ibisate, S. John, S. W. Leonard, C. Lopez, F. Meseguer, H. Miguez, J. P. Mondia, G. A. Ozin, O. Toader, H. M. van Driel. *Nature* **2000**, *405*, 437.

[3] M. Fujita, S. Takahashi, Y. Tanaka, T. Asano, S. Noda . *Science* **2005**, *308, 1296.*

[4] P. Lodahl, A. F. van Driel, I.S. Nikolaev, A. Irman, K. Overgaag, D. L. Vanmaekelbergh, W. Vos, *Nature* **2004**, *430*, 654.

[5] R.F Oulton, V.J. Sorger, T. Zentgraf, R. Ma, C. Gladden, L. Dai, G. Bartal, X. Zhang, *Nature* **2009**, *461*, 629.

[6] J. Grandidier, S.Massenot, G. Colas des Francs, A.Bouhelier, J.C. Weeber, L. Markey, A.Dereux, J. Renger, M.U.Gonzalez, R.Quidant, *Phys. Rev. B* **2008**, *78*, 245419.

[7] T.A. Kelf, Y.Sugawara, J.J. Baumberg, M.Abdelsalam, P.N.Barlett, *Phys. Rev. Lett.* **2005,** *95*, 116802.

[8] G. Vecchi, V. Giannini, J.G. Rivas, *Phys. Rev. Lett.* **2009**, *102*, 146807.

[9] M. López-García, J.F.Galisteo.-Lopez, A. Blanco, J. Sánchez-Marcos, C. López, A. García-Martín, *Small* **2010**, in press.

[10] J. Sun, C. Tang, P. Zhan, Z. Han, A. Cao, Z. Wang, *Langmuir* **2010**, *26*, 7859.

[11] Y. Li, W. Cai, and G. Duan, Chem. Mater. **2007**, *20*, 615.

[12] R.M Cole, J.J Baumberg, F.J Garcia de Abajo, S. Mahajan, M. Abdelsalam, P.N. Bartlett, *Nano Lett.* **2007**, *7*, 2094.

[13] H. Miyazaki, K. Ohtaka, *Phys. Rev. B* **1998**, *58*, 6920.

[14] R. M. Cole, Y. Sugawara, J. J. Baumberg, S. Mahajan, M. E. Abdelsalam, P. Barlett, . *Phys. Rev. Lett.* **2006**, *97*, 137401.

[15] L. Shi, X. Liu, H. Yin, J. Zi, *Phys. Lett. A.* **2009**, *374*, 1059.

[16] X. Yu, L. Shi, D. Han, J. Zi, P.V. Braun, *Adv .Funct. Mater.* **2010**, *20*, 1910.

[17] L. Landström, D. Brodoceanu, D. Bäuerle, F.J. Garcia-Vidal, S.G. Rodrigo and L. Martin-Moreno, *Optics Express* **2009**, *17*, 761.

[18] D. Pacifici, J. Henri, H.A. Atwater, *Nature Phot.* **2007,** *1*, 402.

[19] P.R Evans, G.A Wurtz, W.R Hendren, R. Atkinson, W. Dickson, A.V Zayats, R.J Pollard, *Appl. Phys Lett*, **2007,** *91*, 043101.

[20] V.V. Temnov, G. Armelles, U. Woggon, D. Guzatov, A. Cebollada, A. Garcia-Martin, J.M Garcia-Martin,T. Thomay, A. Leitenstorfer, R. Bratschitsch, *Nature Phot.* **2010**, *4*, 107.

[21] J. B. González-Díaz, A. García-Martín, G. Armelles, J.M García-Martín, C.Clavero, A. Cebollada, R.A Lukaszew, J.R Skuza, D.P Kumah, R. Clarke, *Phys. Rev. B* **2007**, *76*, 153402.

[22] D. Gérard, V. Laude, B. Sadani, A. Khelif, D. Van Labeke, B. Guizal, *Phys. Rev. B* **2007**, *76*, 235427.

[23] S. Furumi, H. Fudouzi, T. Sawada, *Laser & Photon. Rev.* **2009**, *4*, 205.

[24] T. Fujimura, T. Tamura, T. Itoh, C. Haginoya, Y Komori, T. Koda, *Applied Physics Letters*, **2001**, *78*, 1478

[25] A. Plettl, F.Enderle, M. Saitner, Achim Manzke, C. Pfahler, S. Wiedemann,P. Ziemann, *Adv. Funct. Mater.* **2009**, *19*, 1.

[26] G. von Freymann, S. John, V. Kitaev, G. A. Ozin, *Adv. Mater.* **2005**, 17, 1273.

[27] T. Ding, K. Song, K. Clays, C-H. Tung, *Langmuir* **2010**, 26, 4535.

[28] C. Haginoya, M. Ishibashi, K. Koike, *Applied Physics Letters*, **1997**, *71*, 2934.

[29] P. Jiang, J.F. Bertone, K.S. Hwang, V. L.Colvin, *Chem. Mater.* **1999**, *11*, 2132.